Carbohydrate Polymers 86 (2011) 1113–1117

Contents lists available at ScienceDirect

Carbohydrate Polymers

journal homepage: www.elsevier.com/locate/carbpol

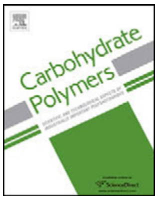

Synthesis and characterization of temperature sensitive hemicellulose-based hydrogels

J.Y. Yang, X.S. Zhou*, J. Fang

State Key Laboratory Pulp and Paper Engineering, South China University of Technology, Guangzhou 510640, China

ARTICLE INFO

Article history:
Received 19 January 2011
Received in revised form 17 May 2011
Accepted 24 May 2011
Available online 7 June 2011

Keywords:
Hydrogel
Polysaccharide
Cross-linking
Electron microscopy
Swelling
Drug delivery

ABSTRACT

Temperature sensitive hemicellulose-based hydrogels were synthesized using hemicellulose obtained from acetic acid pulping of eucalyptus and N-isopropylacrylamide (NIPAAm) through UV photo-crosslinking. Firstly, a derivative of hemicellulose (Hce-MA) containing vinyl bonds within the side chains was prepared by grafting maleic anhydride (MA) to hemicellulose. The Hce-MA was then photo-crosslinked with NIPAAm in LiCl/DMF solvent using UV light to form the hydrogels. The lower critical solution temperature (LCST) and the morphology of the hydrogels were investigated by DSC and SEM, respectively. The LCST of the well-defined honeycomb-like hydrogels was found to increase with the content of Hce-MA. The swelling and de-swelling behaviors of the hydrogels under different temperatures were studied as well. The equilibrium swelling ratio and morphology of the hydrogels were dependent on environment temperature, implying their potential as smart materials for medical application.

1. Introduction

Hydrogels are materials composed of hydrophilic polymers through chemical or physical crosslinking, which can absorb and retain large volume of water in its three-dimensional network without dissolution (Kim, Won, & Chu, 1999a; Park, Shalaby, & Park, 1993). Hydrogels, especially the temperature sensitive ones, are widely studied due to their widespread applications in many fields, such as immobilization of enzyme (Kondo & Fukuda, 1997) and drug delivery (Liu & Chan, 2009). Among these hydrogels, poly N-isopropylacrylamide (PNIPAAm) has attracted extensive interest because its LCST is 32 °C, which is near the human body temperature. Its LCST can be manipulated by introducing hydrophilic/hydrophobic groups (Takei et al., 1993). For instance, an introduction of natural polysaccharides can not only cause a change of LCST, but also improve the biodegradable property of the hydrogels.

Recently, natural polysaccharides, e.g., chitin (Zhao, Mitomo, Nagasawa, Yoshii, & Kumeet, 2003), xanthan gum (Gils, Ray, & Sahoo, 2009), and dextran (Zhang, Wu, & Chu, 2004), have been widely utilized for preparing hydrogels owing to their non-toxic, biodegradable natures and abundant sources. Zhao et al. (2003) prepared a chitin-based hydrogels by radiation synthesis via carboxymethylchitin (CM-chitin). The hydrogels exhibited excellent mechanical properties and swelling property in water. Zhang et al. (2004) synthesized a partially biodegradable, temperature and pH responsive Hce-MA/PNIPAAm hydrogels from dextran and NIPAAm. The LCST increased with the increasing Hce-MA contents.

Hemicelluloses are commonly defined as non-cellulose cell-wall heterogeneous polysaccharides, which normally occur in plant tissues together with cellulose. With a growing environmental concern, interest has evoked among material scientists in hemicelluloses as renewable raw materials for value-added products, such as xylitol, sugar-based polyesters and hydrogels. An interesting feature is that different functionalities can be easily incorporated by physical or chemical crosslinked in the network giving rise to stimuli-responsive physical properties (typically temperature- or pH-sensitive) (Ebringerová, Hromádková, & Heinze, 2005; Gabrielii, Gatenholm, Glasser, Jain, & Kenne, 2000; Huang, Ramaswamy, Tschirner, & Ramarao, 2008). Voepel et al. (2009) synthesized a neutral hydrogel from acetylated galactoglucomannan (AcGGM) and hemicellulose originating from softwood, using hydroxyethyl methacrylate coupled via carbonyldiimidazole and a co-monomer in a radical-initiated polymerization. The hydrogels showed drug release kinetics that could be easily regulated by changing the relative amount of AcGGM.

In this paper, hemicellulose and PNIPAAm were used to prepare temperature sensitive hydrogels. The chemical structures of the hemicellulose, Hce-MA and the resulting hydrogels were investigated using FT-IR and ^{1}H NMR. The morphology, LCST and swelling ratio and deswelling kinetics of the hydrogels were also characterized.

---

* Corresponding author. Tel.: +86 20 22236559; fax: +86 20 22236559.
E-mail address: xszhou@scut.edu.cn (X.S. Zhou).

0144-8617/$ – see front matter © 2011 Elsevier Ltd. All rights reserved.
doi:10.1016/j.carbpol.2011.05.043

2. Materials and methods

2.1. Materials

Eucalyptus (Myrtaceae) obtained from Guangxi, China, was cut into 2 cm × 2 cm chips and dried at 60 °C in an oven overnight. N-isopropylacrylamide (NIPAAm), lithium hydroxide (LiOH), N,N′-methylenebisacrylamide (BIS), 2,2′-dimethoxy-2-phenyl acetophenone (DMPA), N-methylpyrrolidone (NMP) were commercial products of Aladdin (Sigma–Aldrich Biotechnology, L. R.) Reagent Inc, China, Maleic anhydride (MA), dimethyl formamide (DMF) and lithium chloride (LiCl) were obtained from Kermel Reagent Inc, China, and dehydrated with 5A molecular sieve prior to be used.

2.2. Preparation of hemicellulose

The major components of wood were isolated by acetic acid pulping (Gabrielii et al., 2000). The eucalyptus chips were pretreated by 90% acetic acid at 105 °C for 2 h, and then cooked in 90% acetic acid (ratio of liquor to chips is 6) catalyzed by 3% H_2SO_4 (w/w, on chips) at 105 °C for 3 h. The pulped liquor was concentrated and added into sextuple water, the resulting deposit was acetic acid lignin. After filtration, the polysaccharide liquor was precipitated by ethanol and further freeze-dried to obtain solid hemicellulose (Hce, Mw 4693 – determined with GPC).

2.3. Synthesis of hemicellulose derivatives (Hce-MA)

1 g of Hce was dissolved in a flask containing 90 ml of LiCl/DMF mixed solvent at 90 °C. After the solution was cooled down to 60 °C, LiOH catalyst was added and stirred for 15 min, followed by the slow addition of MA. The reaction was conducted at 60 °C in the flask for 10 h under nitrogen atmosphere. The product was precipitated with isopropyl alcohol at a low temperature as 10 °C, filtered, and then freeze-dried under vacuum at −50 °C for 1 day. The degree of substitution (DS) of Hce-MA precursor was estimated by ^{1}H NMR (DRX-400, BRUKER Company, USA) using D_2O as a solvent (Voepel et al., 2009).

2.4. Preparation of hydrogels

Hce-MA and $\text{NIPAAm}_{[0]}$ with different ratios (listed in Table 1) were dissolved in de-ionized water to make the solutions which concentration were all kept in 25% (w/v). The photo-initiator (DMPA, 6% on Hce-MA and NIPAAm) dissolved in NMP solvent was added to the precursor solution. The solution was then irradiated by a long-wavelength UV lamp (365 nm, 100 W) for 10 h. The resultant hydrogels were immersed in de-ionized water at room temperature for 48 h to remove the unreacted chemicals.

The PNIPAAm hydrogel (NIP) was also synthesized for comparison. 1 g NIPAAm and 0.02 g crosslinker (BIS) were dissolved in 4 ml de-ionized water, and then irradiated with DMPA by UV for 10 h. The hydrogel was purified according to the same method addressed above.

2.5. FT-IR analyses

The FT-IR spectra of hydrogels were obtained with a Nexus 470 spectrophotometer (Thermo Nicolet, USA). Prior to the measurement, the hydrogels were immersed in de-ionized water at ambient temperature for 4 h to ensure the reaching of the maximum swelling ratio; then the swollen hydrogel samples were immersed into a hot water (50 °C) bath for 2 h to shrinkage and dried in a vacuum oven at 40 °C for 12 h. The dried hydrogel was milled into powder and analyzed by KBr pellet method in the wavelength region of 4000–500 cm^{-1}.

2.6. Thermo-behavior of the hydrogels

The LCST of the hydrogels were determined by DSC using a Q200 apparatus (TA Instruments, USA). The swollen hydrogel samples were analyzed from 0 to 45 °C under N_2 atmosphere with a flow rate of 25 ml min^{-1} and the heating rate at 10 °C min^{-1}.

2.7. Interior morphology of the hydrogels

The swollen hydrogel samples were quickly frozen and fractured carefully in liquid nitrogen, and then freeze-dried in a Freeze Drier (ModulyoD, USA) under vacuum at −50 °C for 1 day to completely remove the water in the network of hydrogels. The samples sputter-coated with gold were then observed by SEM (Hitachi S3700, Japan).

2.8. Temperature dependence of the hydrogels

The hydrogel samples were immersed into water at the temperature ranging from 25 to 37 °C for 4 h to permit the maximum swollen. Then they were removed from water and weight after wiping away the surface water with moistened filter paper. The maximum swelling ratio is defined as the weight of water in maximal swollen hydrogel (W_s) per dried weight of hydrogel (W_d) before swelling.

HMN4 containing more Hce-MA is more hydrophilic than HMN1–3 and difficult to reach its equilibrium swollen. Thus the maximum swelling ratios of HMN4 before it dissolved or dissociated in water were measured.

2.9. Swelling and de-swelling kinetics of the hydrogels

The above gravimetric method was also employed to study the swelling and de-swelling kinetics of the hydrogels. The swelling behaviors of the dried hydrogels were measured at 25 °C. The sample was taken out from 25 °C water at regular time intervals and weighted. The water uptake is defined as $100 \times [(W_t - W_d)/W_s]$, where W_t is the weight of wet hydrogel at a given time interval and the other symbols are the same as above.

To explore the de-swelling kinetics of the hydrogels, the swollen hydrogels were transferred from 25 °C to 40 °C distilled water bath for predetermined durations, and the weight changes were measured and recorded. The water retention is defined as $100 \times [(W_t - W_d)/W_s]$, the symbols are the same as above.

3. Results and discussion

3.1. Synthesis of Hce-MA/PNIPAAm hydrogels

The procedure of the HMN hydrogel preparation is shown in Fig. 1. Hemicellulose was firstly modified by MA through esterification reaction to form a hemicellulose derivative (Hce-MA, DS = 1.0) containing vinyl groups in the side chains. Thus the HMN hydrogel was obtained by photocrosslinking of the unsaturated functional groups in Hce-MA and NIPAAm.

Among the HMN series, HMN5 having higher hydrophilic Hce-MA content was easily disassociated in water within 24 h, thus it was unable to be characterized as below methods.

3.2. FT-IR spectra of Hce-MA/PNIPAAm hydrogels

The FT-IR spectra of the hemicellulose derivative (Hce-MA), PNIPAAm and HMN hydrogels are shown in Fig. 2. In case of Hce-MA, a broad absorption peak at 3480 cm^{-1} and the peak presented at

Table 1
Feed compositions of the HMN hydrogels and results of LCST measurement.

Materials and results	Samples					
	NIP	HMN1	HMN2	HMN3	HMN4	HMN5
Hce-MA/%	0	20	30	50	70	80
NIPAAm/%	100	80	70	50	30	20
LCST/°C	32.00	27.44	28.49	30.29	32.12	–

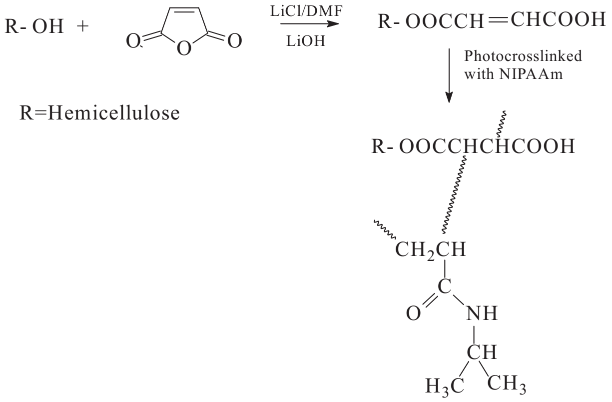

Fig. 1. The scheme of preparation of HMN hydrogels.

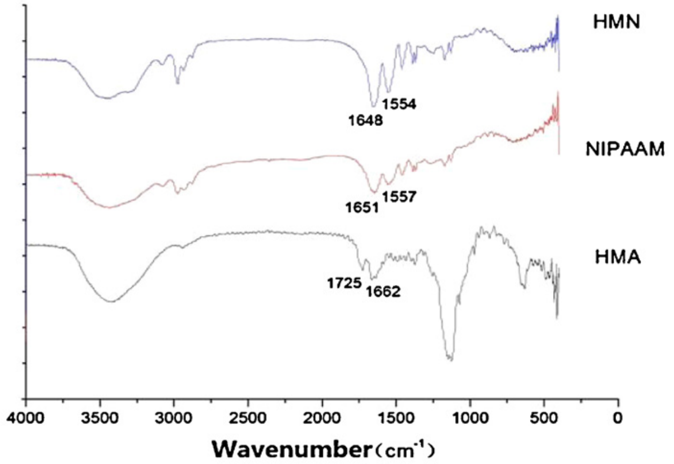

Fig. 2. FT-IR spectra of HCE-MA, PNIPAAm and HMN hydrogels.

1120 cm^{-1} belong to O–H and C–O vibration, respectively. The typical absorption peak of carbonyl group at 1725 cm^{-1} illustrates that MA was introduced into Hce successfully. The bands at 1648 and 1554 cm^{-1} are assigned to the typical amide group in NIPAAm and HMN hydrogels, and the N–H (from NIPAAm) stretching vibration appear a broad band at 3400–3200 cm^{-1}.

3.3. Interior morphology of hydrogels

Fig. 3 shows the SEM images of the cross-section of the freeze-dried hydrogel samples. The HMN hydrogels show a relatively smooth surface with a macropore architecture while the NIP one exhibits a rugged structure. The fraction of double bond crosslinking structure decrease with the absence of Hce-MA leads to the reduction in strength of the networks, resulting to the shrinkage and partial collapse during freeze-drying.

As shown in micrographs of NIP and HMN1 (Fig. 3), the pore structure of the hydrogel is dramatically changed from irregular loose pore structure in NIP hydrogel to well-defined honey-comb

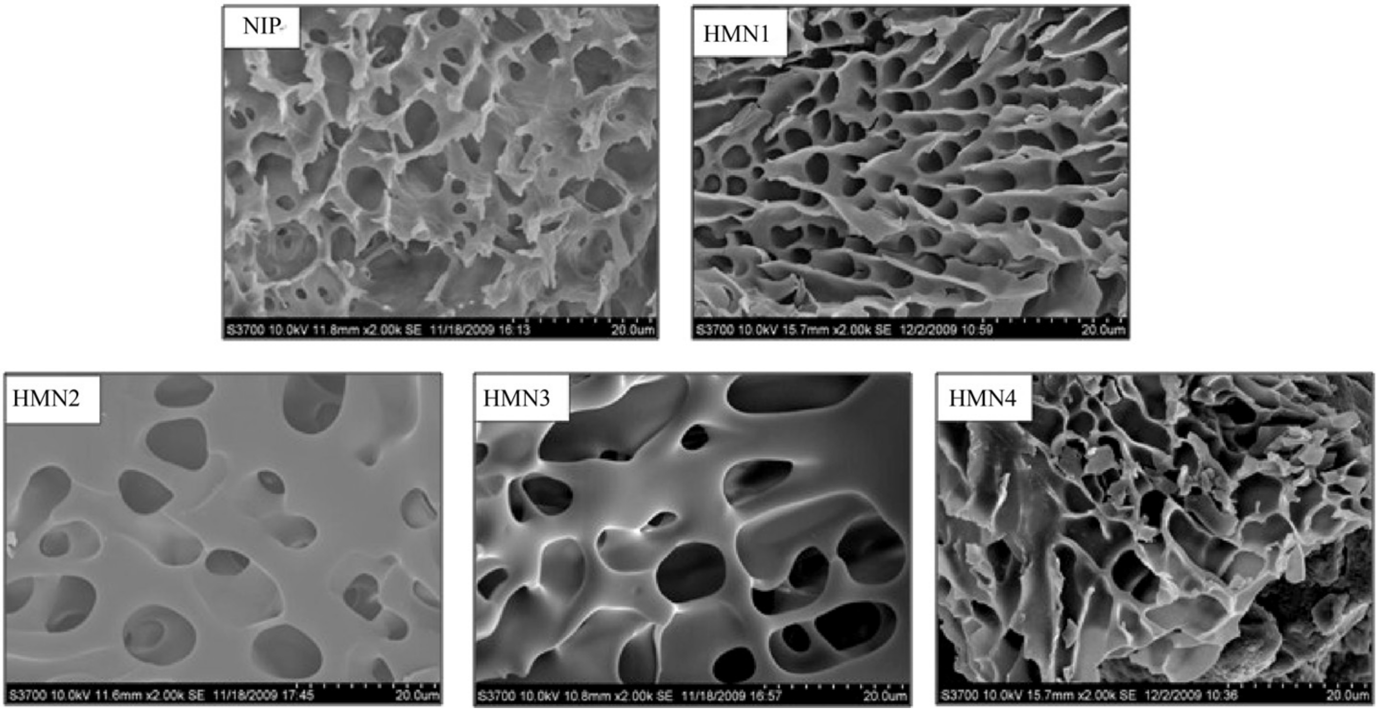

Fig. 3. SEM micrographs of hydrogels.

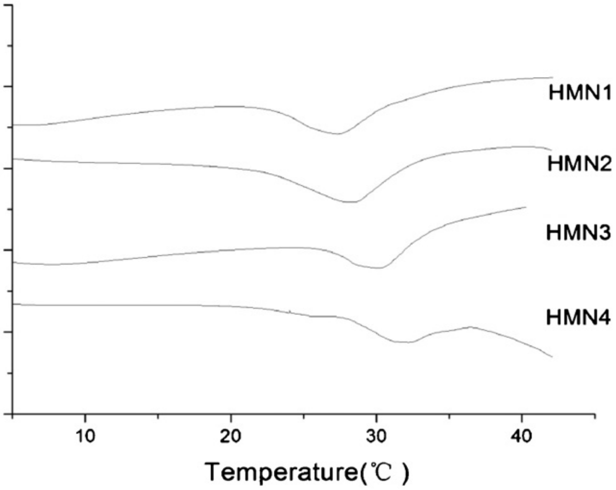

Fig. 4. DSC curves of the HMN hydrogels.

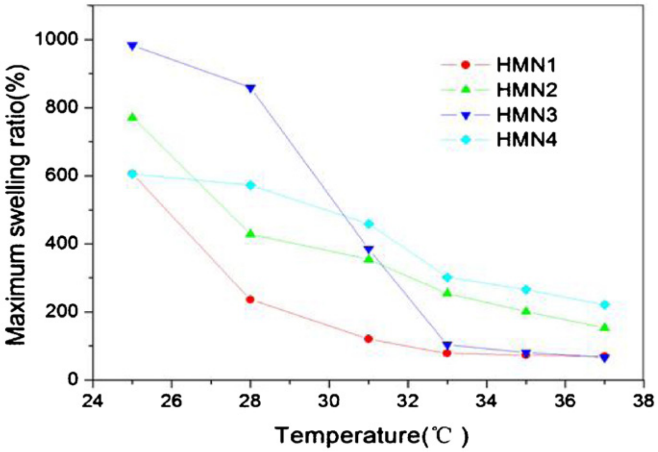

Fig. 5. Maximum swelling ratio of hydrogels at different temperatures.

like structure with stronger walls in HMN1 hydrogel for initial incorporation of Hce-MA into NIPAAm. The pore sizes of the hydrogel increase and the walls become thicker with the increase of Hce-MA content, except for HMN4 which has smaller pores due to the increasing hydrophilicity and crosslinking level. Therefore, the amounts and the velocity of water transporting from the hydrogels HMN2 and HMN3 under the measurement temperature were decreased, compared with those from HMN4. This behavior was further confirmed by the swelling and de-swelling data given later.

3.4. LCST of the HMN hydrogels

The LCST data of the HMN hydrogels determined by DSC (Fig. 4) indicate that the LCST increased with increasing Hce-MA content in the HMN hydrogels due to the hydrophilicity of Hce-MA. It is well known that water exists in polymer networks in three different physical states: free water, intermediate water and bound water (Khalid, Agnely, Yagoubi, Grossiord, & Couarraze, 2002). And there exists a hydrophilic/hydrophobic balance, e.g., the amide and isopropyl group in the NIPAAm unit, in the thermal induced sensitive hydrogels (Pan & Sano, 2005). If the balance is broken by the change of the interaction between the hydrophilic or hydrophobic groups with variation of external temperature, volume-phase transition will happen when free water exhaust, and therefore lead to shrinkage or expansion of the hydrogels. Changes of heat flow reflected in the endothermic peak on DSC curves, which corresponded to LCST of the hydrogels.

Based on the above viewpoints, the improvement of the hydrogen bond with the introduction of hydrophilic Hce-MA should lead to the increase of LCST in the hydrogel. However, the real LCST of HMNs was still lower than that of PNIPAAm hydrogel (32 °C) though the LCST of the samples were increased with the increase of the Hce-MA content. The result maybe generated by the inevitable presence of hydrophobic lignin in the hemicellulose isolated from woods, which led to the decrease of LCST. Moreover, the crosslink generated between hemicellulose derivative (Hce-MA) and NIPAAm in the process of gel formation, meanwhile, the selfpolymerization may happen in Hce-MA and NIPAAm, respectively, which will also result in the close LCST between HMN and PNIPAAm hydrogels.

3.5. Maximum swelling ratio of hydrogels at different temperatures

Fig. 5 demonstrates that the maximum swelling ratio of the HMN hydrogels decreases with increasing environmental temperature, indicating that the HMN hydrogels are thermal responsive as well as PNIPAAm. When external temperature is below LCST, the negative-temperature sensitive hydrogels will absorb more water to expand because there is more hydrogen bond formation between the hydrophilic groups and water in the system. Generally, based on the swelling ratio experiments, the phase transition temperature (LCST) is regarded as the temperature point at which the swelling ratio decreases dramatically (or an inflexion point occurs) (Kim, Won, & Chu, 1999b). The LCST of HMN1–4 estimated from the equilibrium swelling ratio profiles in Fig. 5 are approximately 28, 28, 30 and 32 °C, respectively, which are in agreement with DSC measurement ($\text{LCST}_{\text{HMN1–4}}$ = 27.44, 28.49, 30.29 and 32.12 °C, respectively).

The maximum swelling ratio of HMN hydrogels increased with Hce-MA content. The swelling ratio of HMN4 still related to the temperature, but not as dramatically as other HMNs, which is probably ascribed to its higher crosslinking level and closed channel in the network.

3.6. Swelling and de-swelling behaviors

The swelling rate at 25 °C of the dried hydrogels was found to increase with the content of Hce-MA as shown in Fig. 6. The swelling ratio of HMN4 increased at a fast rate during the first

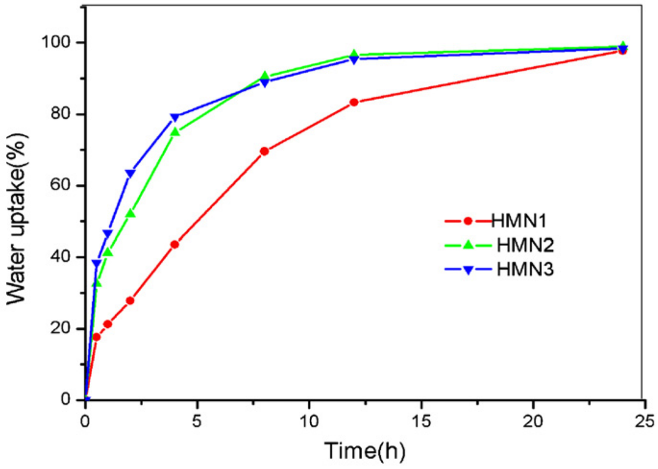

Fig. 6. Swelling behaviors of hydrogels at 25 °C.

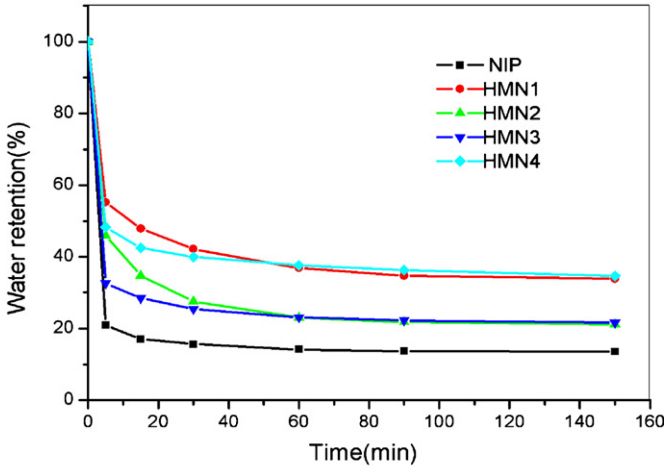

Fig. 7. De-swelling behaviors of hydrogels at 40 °C.

8 h and then started to dissolve without achieving equilibrium. This is attributed to the higher hydrophilicity of HMN hydrogels having higher Hce-MA content, which causes more hydrogen bonds with water molecules and thus a faster water uptake rate.

The de-swelling behaviors of hydrogels are shown in Fig. 7. When the external temperature increased from 25 °C to 40 °C, the volume-phase transition happened, thus inducing the swelled hydrogels to extrude the absorbed water and shrink. However, it was found that the de-swelling rate of HMN hydrogels was lower than that of PNIPAAm hydrogel due to the fact that the thermo-responsive property is diluted with the incorporation of the non-thermo-responsive species like Hce-MA into the hydrogels.

The fact that HMN2 and HMN3 showed a faster response rate than HMN1 and HMN4, is inconsistent with the above diluted viewpoints and different from the de-swelling behaviors of dextran–NIPAAm hydrogels (DMN) as reported by Zhang et al. (2004). The response rate of the DMN hydrogels increased with the dextran content, suggesting that the de-swelling rate is controlled by two opposite factors, dilution and weaken skin layer. In the previous PNIPAAm study (Kaneko & Yoshida, 1995; Pan & Sano, 2005; Zhang, Bhat, & Jandt, 2009), a dense skin layer was formed on the surface of PNIPAAm hydrogel in the shrinking process, which could restrict the free water to diffuse out due to the poor water-permeability of the dense layer, leading to bubble formation. Only after the breaking of these bubbles, the free water could be released. Herein, hydrophilic polymer introduced into PNIPAAm networks could not only weaken the dense layer, but also act as water-releasing channels. Nevertheless, the other potential influencing factors such as the pore structure of the hydrogels should be considered. The NIP and HMN hydrogels have different pore structure as shown in Fig. 3, resulting in different water-releasing channels. HMN2 and HMN3 had the pore size larger than HMN1 and HMN4, which is more propitious to water-releasing. Overall, the response rate of the HMN hydrogels is controlled by the synergistic effect of the three factors, thermal responsive moiety, formation of dense skin layer and the pore size of the hydrogels.

4. Conclusions

Hydrogels consisting of polysaccharide (hemicellulose derivative, Hce-MA) and NIPAAm were synthesized by UV photo-crosslinking. The resulting HMN hydrogels were temperature sensitive. The equilibrium swelling ratio in water decreased with the increase of the external temperature. The pore size of the hydrogels increased and the pore structure became well-defined honeycomb-like when hydrophilic component (Hce-MA) was introduced. The LCST increased with increasing Hce-MA content, and a faster water uptake rate appeared. These properties are controllable by manipulating the ratios of Hce-MA and NIPAAm, permitting the hydrogels to be promising materials for biomedical application.

Acknowledgments

The financial support from Hi-Tech Research and Development Program of China (Contract Grant Number: 2007AA100704) is greatly appreciated.

References

Ebringerová, A., Hromádková, Z., & Heinze, T. (2005). Hemicellulose. *Advances in Polymer Science*, *186*, 1–3.

Gabrielii, I., Gatenholm, P., Glasser, W. G., Jain, R. K., & Kenne, L. (2000). Separation, characterization and hydrogel-formation of hemicellulose from aspen wood. *Carbohydrate Polymers*, *43*, 367–374.

Gils, P. S., Ray, D., & Sahoo, P. K. (2009). Characteristics of xanthan gum-based biodegradable superporous hydrogel. *Journal of Biological Macromolecules*, *45*, 364–371.

Huang, H. J., Ramaswamy, S., Tschirner, U. W., & Ramarao, B. V. (2008). A review of separation technologies in current and future biorefineries. *Separation and Purification Technology*, *62*, 1–21.

Kaneko, Y, & Yoshida, R. (1995). Temperature-responsive shrinking kinetics of poly(N-isopropylacrylamide) copolymer gels with hydrophilic and hydrophobic comonomers. *Journal of Membrane Science*, *101*, 13–22.

Khalid, M. N., Agnely, F., Yagoubi, N., Grossiord, J. L., & Couarraze, G. (2002). Water state characterization, swelling behavior, thermal and mechanical properties of chitosan based networks. *European Journal of Pharmaceutical Sciences*, *15*, 425–432.

Kim, S. H., Won, C. Y., & Chu, C. C. (1999a). Synthesis and characterization of dextran-maleic acid based hydrogel. *Journal of Biomedical Materials Research*, *46*, 160–170.

Kim, S. H., Won, C. Y., & Chu, C. C. (1999b). Synthesis and characterization of dextran-based hydrogel prepared by photocrosslinking. *Carbohydrate Polymers*, *40*, 183–190.

Kondo, A., & Fukuda, H. (1997). Preparation of thermo-sensitive magnetic hydrogel microspheres and application to enzyme immobilization. *Journal of Fermentation and Bioengineering*, *84*(4), 337–341.

Liu, Y. X., & Chan, M. B. (2009). Hydrogel based on interpenetrating polymer networks of dextran and gelatin for vascular tissue engineering. *Biomaterials*, *30*, 196–207.

Pan, X. J., & Sano, Y. (2005). Fractionation of wheat straw by atmospheric acetic acid process. *Bioresource Technology*, *96*, 1256–1263.

Park, K., Shalaby, W. S. W., & Park, H. (1993). Biodegradable hydrogels for drug delivery. *Lancaster*, *11*, 59–84.

Takei, Y. G., Aoki, T., Sanui, K., Ogata, N., Okano, T., & Sakurai, Y. (1993). Temperature-responsive bioconjugates. 2. Molecular design for temperature-modulated bioseparations. *Bioconjugate Chemistry*, *4*(5), 341–346.

Voepel, J., Sjoberg, J., Reif, M., Albertsson, A. C., Hultin, U. K., & Gasslander, U. (2009). Drug diffusion in neutral and ionic hydrogels assembled from acetylated galactoglucomannan. *Journal of Applied Polymer Science*, *112*, 2401–2412.

Zhang, J. T., Bhat, R., & Jandt, K. D. (2009). Temperature-sensitive PVA/PNIPAAm semi-IPN hydrogels with enhanced responsive properties. *Acta Biomaterials*, *5*, 488–497.

Zhang, X. Z., Wu, D. Q., & Chu, C. C. (2004). Synthesis and characterization of partially biodegradable, temperature and pH sensitive HCE-MA/PNIPAAm hydrogels. *Biomaterials*, *25*, 4719–4730.

Zhao, L., Mitomo, H., Nagasawa, N., Yoshii, F., & Kumeet, T. (2003). Radiation synthesis and characteristic of the hydrogels based on carboxymethylated chitin derivatives. *Carbohydrate Polymers*, *51*, 169–175.